Parametrization of the Contribution of Mono- and Bidentate Ligands on the Symmetric C≡O Stretching Frequency of *fac*-[Re(CO)$_3$]$^+$ Complexes

Fabio Zobi*

Institute of Inorganic Chemistry, University of Zürich, Winterthurerstrasse 190, CH-8057 Zürich, Switzerland

A ligand parameter, $IR_P(L)$, is introduced in order to evaluate the effect that different monodentate and bidentate ligands have on the symmetric C≡O stretching frequency of octahedral d^6 *fac*-[Re(CO)$_3$L$_3$] complexes (L = mono- or bidentate ligand). The parameter is empirically derived by assuming that the electronic effect, or contribution, that any given ligand L will add to the *fac*-[ReCO$_3$]$^+$ core, in terms of the total observed energy of symmetric C≡O stretching frequency ($\nu_{CO^{obs}}$), is additive. The $IR_P(CO)$ (i.e., the IR_P of carbon monoxide) is first defined as one-sixth that of the observed C≡O frequency ($\nu_{CO^{obs}}$) of [Re(CO)$_6$]$^+$. All subsequent $IR_P(L)$ parameters of *fac*-[Re(CO)$_3$L$_3$] complexes are derived from $IR_P(L) = {}^1/_3[\nu_{CO^{obs}} - 3IR_P(CO)]$. The symmetric C≡O stretching frequency was selected for analysis by assuming that it alone describes the "average electronic environment" in the IR spectra of the complexes. The $IR_P(L)$ values for over 150 ligands are listed, and the validity of the model is tested against other octahedral d^6 *fac*-[M(CO)$_3$L$_3$] complexes (M = Mn, ^{99}Tc, and Ru) and *cis*-[Re(CO)$_2$L$_4$]$^+$ species and by calculations at the density functional level of theory. The predicted symmetric C≡O stretching frequency ($\nu_{CO^{cal}}$) is given by $\nu_{CO^{cal}} = S_R[\sum IR_P(L)] + I_R$, where S_R and I_R are constants that depend upon the metal, its oxidation state, and the number of CO ligands in its primary coordination sphere. A linear relationship between IR_P values and the well-established ligand electrochemical parameter E_L is found. From a purely thermodynamic point of view, it is suggested that ligands with high $IR_P(L)$ values should weaken the M−CO bond to a greater extent than ligands with low $IR_P(L)$ values. The significance of the results and the limitations of the model are discussed.

Introduction

In recent years, it has been recognized that carbon monoxide (CO) plays a fundamental role in humans as a small-molecule messenger.[1] Its physiological functions have not yet been fully understood, but a large body of evidence suggests that CO acts as a signaling molecule in the inducible defensive system against stressful stimuli, including UVA radiation, carcinogens, and several other conditions generally characterized by the production of oxygen free radicals.[1] There is a large growing interest in the medicinal applications of CO. The vasorelaxant and vasodilatatory properties of the gaseous molecule have been well documented,[2−5] and it has been shown that CO possesses properties that make it potentially useful in cardiac transplants.[6−13]

Because the importance of CO is been increasingly recognized, there is a steadily growing interest in the synthesis and design of CO-releasing molecules (CORMs) as stable solid storage of CO for potential therapeutic applications.[14−20]

*To whom correspondence should be addressed. E-mail: fzobi@aci.uzh.ch.

(1) Wu, L.; Wang, R. *Pharmacol. Rev.* **2005**, *57*, 585–630.
(2) Clark, J. E.; Naughton, P.; Shurey, S.; Green, C. J.; Johnson, T. R.; Mann, B. E.; Foresti, R.; Motterlini, R. *Circ. Res.* **2003**, *93*, e2–8.
(3) Grilli, A.; De Lutiis, M. A.; Patruno, A.; Speranza, L.; Gizzi, F.; Taccardi, A. A.; Di Napoli, P.; De Caterina, R.; Conti, P.; Felaco, M. *Ann. Clin. Lab. Sci.* **2003**, *33*, 208–215.
(4) Guo, Y.; Stein, A. B.; Wu, W. J.; Tan, W.; Zhu, X.; Li, Q. H.; Dawn, B.; Motterlini, R.; Bolli, R. *Am. J. Physiol. Heart Circ. Physiol.* **2004**, *286*, H1649–1653.
(5) Liu, H.; Song, D.; Lee, S. S. *Am. J. Physiol. Gastrointest. Liver Physiol.* **2001**, *280*, G68–74.
(6) Brian, J. E., Jr.; Heistad, D. D.; Faraci, F. M. *Stroke* **1994**, *25*, 639–643.
(7) Coceani, F.; Breen, C. A.; Lees, J. G.; Falck, J. R.; Olley, P. M. *Circ. Res.* **1988**, *62*, 471–477.
(8) Gagov, H.; Kadinov, B.; Hristov, K.; Boev, K.; Itzev, D.; Bolton, T.; Duridanova, D. *Pfluegers Arch.* **2003**, *446*, 412–421.

(9) Graser, T.; Vedernikov, Y. P.; Li, D. S. *Biomed. Biochim. Acta* **1990**, *49*, 293–296.
(10) Kozma, F.; Johnson, R. A.; Zhang, F.; Yu, C.; Tong, X.; Nasjletti, A. *Am. J. Physiol.* **1999**, *276*, R1087–1094.
(11) McGrath, J. J.; Smith, D. L. *Proc. Soc. Exp. Biol. Med.* **1984**, *177*, 132–136.
(12) Ndisang, J. F.; Tabien, H. E.; Wang, R. *J. Hypertens.* **2004**, *22*, 1057–1074.
(13) Wang, R. *Can. J. Physiol. Pharmacol.* **1998**, *76*, 1–15.
(14) Foresti, R.; Bani-Hani, M. G.; Motterlini, R. *Intensive Care Med.* **2008**, *34*, 649–658.
(15) Varadi, J.; Lekli, I.; Juhasz, B.; Bacskay, I.; Szabo, G.; Gesztelyi, R.; Szendrei, L.; Varga, E.; Bak, I.; Foresti, R.; Motterlini, R.; Tosaki, A. *Life Sci.* **2007**, *80*, 1619–1626.
(16) Sawle, P.; Hammad, J.; Fairlamb, I. J.; Moulton, B.; O'Brien, C. T.; Lynam, J. M.; Duhme-Klair, A. K.; Foresti, R.; Motterlini, R. *J. Pharmacol. Exp. Ther.* **2006**, *318*, 403–410.
(17) Motterlini, R.; Clark, J. E.; Foresti, R.; Sarathchandra, P.; Mann, B. E.; Green, C. J. *Circ. Res.* **2002**, *90*, E17–24.
(18) Motterlini, R.; Mann, B. E.; Foresti, R. *Expert Opin. Invest. Drugs* **2005**, *14*, 1305–1318.
(19) Motterlini, R.; Mann, B. E.; Johnson, T. R.; Clark, J. E.; Foresti, R.; Green, C. J. *Curr. Pharm. Des.* **2003**, *9*, 2525–2539.
(20) Motterlini, R.; Sawle, P.; Hammad, J.; Bains, S.; Alberto, R.; Foresti, R.; Green, C. J. *FASEB J.* **2005**, *19*, 284–286.
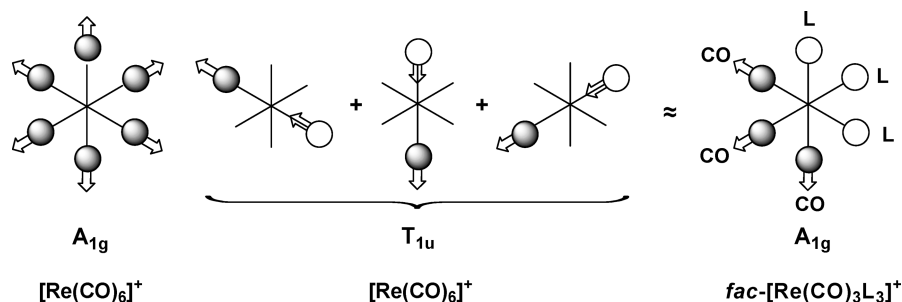
Figure 1. Symmetry species of CO stretching modes of $[ReCO_6]^+$ and fac-$[Re(CO)_3L_3]^+$.

An obvious choice for CORMs is transition-metal complexes with one or more CO ligands. One important example of a metal-based CORM is the fac-[RuCl(glycinato)(CO)$_3$] complex (CORM-3).[21–23] At present, CORM-3 is one of the most promising compounds for CO release in vivo and its chemistry and therapeutic effects are well understood.[21–23]

It has been pointed out that, from a purely thermodynamic point of view, CO cleavage from metal complexes can be the result of a weak M—CO bond.[24] A high CO stretching frequency in the IR spectrum of a compound is a good indication for a weak M—CO bond. The higher the CO stretching frequency, the weaker is the M → CO π-back-donation and the weaker is the double-bond character of the covalent M—C bond. There is, however, no simple model to predict what effect different mono- and bidentate ligands will have on the CO stretching frequencies of a metal carbonyl complex. Consequently, from a medicinal point of view, there is no simple way of rationally designing potentially useful metal complexes with high CO frequencies as a general indication of a labile M—CO bond. A mathematical prediction of the CO frequencies of any given $[M(CO)_n]$ core would serve as a useful guide for the design of novel CORMs, based purely on the thermodynamic assumption mentioned above.

Several theoretical models have been developed in the past in order to relate ligand effects to vibrational spectroscopy.[25–30] All of these models are based on a mathematical evaluation of C—O force constants according, to some extent, to the general approach originally described by Cotton and Kraihanzel.[25–27] Generally, only monodentate ligands (most often phosphines) have been considered, and their effect has been evaluated mainly on pentacarbonyl complexes. These models have been commonly accepted, but only a few ligands have been parametrized.

Nevertheless, the common basis of all of the models is the concept of an "average environment" or that ligand effects are additive. On the same basis, we introduce here a ligand parameter, $IR_P(L)$, in order to generate a ligand series that may be used to predict the symmetric C≡O stretching frequency of octahedral d^6 fac-[Re(CO)$_3$L$_3$] complexes (L = mono- or bidentate ligand) and other metal ions that are of potential use as CORMs. The parameter, which was empirically derived from the evaluation of the IR spectra of a large number of fac-[Re(CO)$_3$L$_3$] complexes, was obtained under the following assumptions:

1. *In a fac-[Re(CO)$_3$L$_3$] species, the symmetric C≡O stretching frequency alone ($\nu_{CO^{obs}}$) describes the "average electronic environment" in the IR spectra of the complex.* With this statement it is assumed that, in a fashion similar to what Bigorgne has described,[31] for any given fac-[Re(CO)$_3$L$_3$] complex, the electronic contribution brought about from the ligands, in terms of both σ and π bonding, is directly transferred to the CO's. Indeed, theoretical calculations will later show that the charge transferred from the three facially arranged L's to the three CO's induces a linear decrease and increase of the Re—C and C—O bond orders, respectively.

2. *The electronic effect, or contribution, that any given ligand L will add to the fac-[ReCO$_3$]$^+$ core, in terms of the total observed energy of symmetric C≡O stretching frequency ($\nu_{CO^{obs}}$), is additive and, as such, can be parametrized.* This assumption does not deserve much comment. Since the original intuition of Tsuchida,[32–34] there is enough theoretical evidence to assume that ligand additivity is widely justifiable.[25–31,35,36]

3. *Rather than A$_{1g}$, the frequency (or energy) of the T$_{1u}$ CO stretching mode of the corresponding [ReCO$_6$]$^+$ complex, more closely approximates the frequency (or energy) of the A$_{1g}$ CO stretching mode of the fac-[ReCO$_3$]$^+$ core* (Figure 1). This is undoubtedly an oversimplification of the problem, but the assumption is derived from the following consideration: the model we are about to describe relies on the initial definition of a CO parameter from which all other ligand parameters are derived. From a mathematical point of view, the only metal carbonyl complex that provides "one unknown and one equation" is the $[ReCO_6]^+$ cation (where unknown = ligand, i.e., CO, and equation = relationship between $\nu_{CO^{obs}}$ and the ligand). However, because of a change in the point

(21) Desmard, M.; Davidge, K. S.; Bouvet, O.; Morin, D.; Roux, D.; Foresti, R.; Ricard, J. D.; Denamur, E.; Poole, R. K.; Montravers, P.; Motterlini, R.; Boczkowski, J. *FASEB J.* **2008**, *23*, 1–9.
(22) Foresti, R.; Hammad, J.; Clark, J. E.; Johnson, T. R.; Mann, B. E.; Friebe, A.; Green, C. J.; Motterlini, R. *Br. J. Pharmacol.* **2004**, *142*, 453–460.
(23) Johnson, T. R.; Mann, B. E.; Teasdale, I. P.; Adams, H.; Foresti, R.; Green, C. J.; Motterlini, R. *Dalton Trans.* **2007**, 1500–1508.
(24) Alberto, R.; Motterlini, R. *Dalton Trans.* **2007**, 1651–1660.
(25) Cotton, F. A. *Inorg. Chem.* **1964**, *3*, 702–711.
(26) Cotton, F. A.; Kraihanzel, C. A. *J. Am. Chem. Soc.* **1962**, *84*, 4432–4438.
(27) Kraihanzel, C. A.; Cotton, F. A. *Inorg. Chem.* **1963**, *2*, 533–540.
(28) Graham, W. A. G. *Inorg. Chem.* **1968**, *7*, 315–321.
(29) Timney, J. A. *Inorg. Chem.* **1979**, *18*, 2502–2506.
(30) Haas, H.; Sheline, R. K. *J. Chem. Phys.* **1967**, *47*, 2996–3012.

(31) Bigorgne, M. *J. Organomet. Chem.* **1964**, *2*, 68–78.
(32) Tsuchida, R. *Bull. Chem. Soc. Jpn.* **1938**, *13*, 388–340.
(33) Tsuchida, R. *Bull. Chem. Soc. Jpn.* **1938**, *13*, 436–450.
(34) Tsuchida, R. *Bull. Chem. Soc. Jpn.* **1938**, *13*, 471–480.
(35) Lever, A. B. P. *Inorg. Chem.* **1990**, *29*, 1271–1285.
(36) Stewart, R. P.; Treichel, P. M. *Inorg. Chem.* **1968**, *7*, 1942–1944.

symmetry (O_h for $[ReCO_6]^+$ and C_{3v} for *fac*-[Re-$(CO)_3L_3$]), the A_{1g} modes cannot be directly compared. We then selected the next lower symmetry species of CO stretching modes in $[ReCO_6]^+$ (T_{1u}), which would more closely resemble the A_{1g} stretching mode of the *fac*-$[ReCO_3]^+$ core (Figure 1). As will become clear later, this approximation does not pose a serious problem.

It should be stated that it is *not* the intent of this study to provide a new theoretical model for the evaluation of metal carbonyl stretching frequencies. The intention is to describe a simple mathematical approach in order to evaluate the effect that different mono- and bidentate ligands will have on the CO stretching frequencies of a metal carbonyl complex relative to each other. Thus, for the development of the approach, we took under no further considerations changes in the point symmetry of the molecules evaluated. These were all considered of *pseudo-C_{3v}* symmetry. Analogously, we did not take into consideration coupling of the symmetric and asymmetric stretching frequencies or possible ligand−ligand interactions. The $IR_P(L)$ parameters herein described are purely empirically derived. Thus, the $IR_P(L)$ ligand values should not be considered in absolute terms. The parameters rather should be regarded as a tool for inorganic chemists to sample from the list, ligand types for the design of carbonyl complexes with specific C≡O stretching frequencies.

Experimental Section

The literature was searched for a large representative number of complexes of the type *fac*-[Re(CO)$_3$L$_3$] with the metal ion in a d^6 configuration. Only monomeric species with mono- and bidentate ligands were included in the pool. IR data of the symmetric C≡O stretching frequency ($\nu_{CO^{obs}}$) were selected according to the following criteria: values were taken as reported if spectra were recorded in a solid pellet (e.g., KBr); a -10 cm^{-1} correction was applied to the reported $\nu_{CO^{obs}}$ values if spectra were recorded in solution. The only exception was made for $[Re(CO)_6]^+$ ($\nu_{CO^{obs}}$ in CH$_3$CN = 2085 cm^{-1}),[37] which provided the basis for the analysis. For all other complexes, the correction was applied regardless of the nature of the solvent. The *Origin* program (version 6.1) was used to plot data and derive equations for the best linear fits.

Computational Details. Geometry optimizations as well as frequency calculations for all molecules were performed at the density functional level of theory (DFT) with the *Gaussian03* program package[38] using the hybrid B3LYP functional[39] in conjunction with the LanL2DZ basis set.[40−42] Pure basis functions (5d, 7f) were used in all calculations. Geometries were fully optimized without symmetry restrictions prior to the frequency calculations and full natural bond order (NBO) analysis. For comparison with the $IR_P(L)$ parameters, Mulliken atomic charges were considered, while bond orders were obtained from the Wiberg bond index matrix in the natural atomic orbital basis after a full NBO analysis.

Results and Discussion

The model was developed in a fashion similar to what Lever has described.[35] The $[Re(CO)_6]^+$ cation was first

considered. A single $\nu_{CO^{obs}}$ is reported[37] in its IR spectrum at 2085 cm^{-1}. As was noted in the Introduction, the $[Re(CO)_6]^+$ $\nu_{CO^{obs}}$ does not correspond to the A_{1g} CO stretching mode, which is IR-forbidden. It actually corresponds to the T_{1u} mode. However, as will become clear later, this approximation does not pose a problem. In the X-ray structure[43] of $[Re(CO)_6]^+$, Re−C bonds vary between 2.0 and 1.9 Å, but it was assumed that all Re−C bonds are identical. The IR_P contribution of carbon monoxide [$IR_P(CO)$] was then defined by $2085/6 = 347.5$ cm^{-1}. This value was taken as a constant for the subsequent evaluation of all $IR_P(L)$. The IR_P parameters of Cl$^-$, Br$^-$, and I$^-$ were then defined from the reported $\nu_{CO^{obs}}$ of the corresponding *fac*-[Re(CO)$_3$X$_3$]$^{2-}$ complexes (where X = halide). These were calculated by

$$IR_P(X) = \frac{1}{3}[\nu_{CO^{obs}} - 3IR_P(CO)] \text{ where X} = \text{halide} \quad (1)$$

The values are 319.2, 318.8, and 318.5 cm^{-1} for Cl$^-$, Br$^-$, and I$^-$, respectively. The values for Cl$^-$ and Br$^-$ were confirmed by three independent sources[44−46] (Supporting Information) and were also considered as constant.

For other monodentate (L) and bidentate (L−L) ligands in combination with one of the halides (X), one may, in general, have data for complexes of the type *fac*-[Re(CO)$_3$(L)$_2$X], *fac*-[Re(CO)$_3$(L)X$_2$] and *fac*-[Re(CO)$_3$(L−L)X]. Where possible, $IR_P(L)$ and $IR_P(L-L)$ values were calculated as the mean average from two or three complexes, always keeping $IR_P(CO)$ and $IR_P(X)$ constant. The formulas applied for each calculation are given by

$$IR_P(L) = \frac{1}{2}[\nu_{CO^{obs}} - 3IR_P(CO) - IR_P(X)]$$

for complexes of the type *fac*-[Re(CO)$_3$(L)$_2$X] $\quad (2)$

$$IR_P(L) = [\nu_{CO^{obs}} - 3IR_P(CO) - 2IR_P(X)]$$

for complexes of the type *fac*-[Re(CO)$_3$(L)X$_2$] $\quad (3)$

$$IR_P(L - L) = \frac{1}{2}[\nu_{CO^{obs}} - 3IR_P(CO) - IR_P(X)]$$

for complexes of the type *fac*-[Re(CO)$_3$(L − L)X] $\quad (4)$

In eq 4, the $^1/_2$ term indicates the contribution of each donor atom in L−L. In this fashion, the $IR_P(L)$ values of 92 ligands were first calculated. Subsequently, these $IR_p(L)$ parameters (with L other than CO) were used for a multi-parameter linear-squares analysis to obtain an average value for $IR_p(CO)$ by using data of 130 complexes. The final average $IR_p(CO)$ value was 347.6 cm^{-1} with a standard deviation of ±0.8 cm^{-1}. This value was then taken as the standard for the reevaluation of all other $IR_P(L)$ parameters. The $IR_P(L)$ values derived from this analysis are listed in Table 1, and the self-consistency of the model was checked

(37) Masi, S.; Top, S.; Jaouen, G. *Inorg. Chim. Acta* **2003,** *350,* 665–668.
(38) Iyengar, S. S.; Frisch, M. J. *J. Chem. Phys.* **2004,** *121,* 5061–5070.
(39) Becke, A. D. *J. Chem. Phys.* **1993,** *98,* 5648–5652.
(40) Hay, P. J.; Wadt, W. R. *J. Chem. Phys.* **1985,** *82,* 270–283.
(41) Hay, P. J.; Wadt, W. R. *J. Chem. Phys.* **1985,** *82,* 299–310.
(42) Wadt, W. R.; Hay, P. J. *J. Chem. Phys.* **1985,** *82,* 284–298.

(43) Bruce, D. M.; Holloway, J. H.; Russell, D. R. *J. Chem. Soc., Dalton Trans.* **1978,** 1627–1631.
(44) Hawkes, M. J.; Ginsberg, A. P. *Inorg. Chem.* **1969,** *8,* 2189–2195.
(45) Alberto, R.; Schibli, R.; Schubiger, P. A.; Abram, U.; Kaden, T. A. *Polyhedron* **1996,** *15,* 1079–1089.
(46) Alberto, R.; Egli, A.; Abram, U.; Hegetschweiler, K.; Gramlich, V.; Schubiger, P. A. *J. Chem. Soc., Dalton Trans.* **1994,** 2815–2820.

Table 1. $IR_P(L)$ Parameter Values (cm^{-1})[a]

ligand (L)	$IR_P(L)^{ref}$	E_L^{35}	ligand (L)	$IR_P(L)^{ref}$	E_L^{35}
1,10-phenanthroline (phen)	328[50−52]	0.26	dimethyl sulfoxide (dmso-O)	323*[53]	*0.47*
1,10-phenanthroline, 2,9-dimethyl	325*[54]	0.20	dimethylphenylphosphine (PMe$_2$Ph)	331[55]	0.34
1,10-phenanthroline, 4,7-dimethyl	325*[54]	0.23	dimethyl sulfide (Me$_2$S)	327[56]	0.31
1,10-phenanthroline-5,6-dione (phd)	329[52,57]	0.28	dipyrido[3,2-a:2′,3′-c]phenazine (dppz)	328[52]	
1,1-bis(dimethylphosphino)ethane (dmpe)	327[58]	0.28	dipyrido[3,2-f:2′,3′-h]quinoxaline (dpq)	332[52]	
1,1-bis(diphenylphosphino)ethane (dppe)	332[58]	0.36	ethylamine	326[59]	
1,1-bis(diphenylphosphino)methane (dppm)	332[58]	0.43	ethylenediamine (en)	323[60]	0.06
1,1-bis(diphenylphosphino)propane (pdp)	333[58]	0.42	fluoride (F$^-$)	312*[61]	−0.42
1,2-bis(4-pyridyl)ethane	322*[62]	0.26	formate	325*[63]	−0.30
1,2-bis(diphenylphosphino)acetylene	334[64]	0.46	hydride (H$^-$)	295*[63]	−0.30
1,2-bis(ethylthio)ethane	331[65]	0.32	hydroxide (OH$^-$)	306[63]	−0.59
1,2-bis(methylthio)ethane ((MeS)$_2$et)	332[66]	0.33	imidazole (Im)	325[67,I]	0.12
1,4,7,10-tetraazaphenanthrene (tap)	330[57]	0.36[b]	imidazole, N-methyl (MeIm)	323[68]	0.08
2,2′-azobispyridine (abpy)	329[52,69]		iodide (I$^-$)	318[44]	−0.24
2,2′-bipyrazine (bpz)	331[70]	0.36	isopropylamine	325[71]	0.05
2,2′-bipyridine (bipy)	328[52]	0.259	n-butyl isocyanide (CNBu^n)[b]	333*[71]	0.45
2,2′-bipyridine, 4,4′,5,5′-tetramethyl	331[72]		nitrate (NO$_3^-$)	319[47,58]	−0.11
2,2′-bipyridine, 4,4′-dicarboxylic acid	331[52]		nitrite (NO$_2^-$)	323[73]	0.02
2,2′-bipyridine, 4,4′-dichloro	326[74]		dimethyl phenylphosphonite (P(OMe)$_2$Ph)	342[55]	
2,2′-bipyridine, 4,4′-dimedthyl (4,4′-Me$_2$bpy)	326[51,75,76]	0.23	phenyl isocyanide (CNPh)	332*[71]	0.41
2,2′-bipyridine, 4,4′-dinitro	328[74]	0.28	pyrazine (pyz)	330[57,62]	0.33
2,2′-bipyridine, 5,5′-dimedthyl (5,5′-Me$_2$bpy)	329*[54,76]		pyrazole	325[77]	0.20
2,2′-bipyrimidine (bpm)	331[52]	0.31	pyrazole (1−)	318[77,78]	−0.24
2,2′-biquinoline (biq)	329*[52]	0.29	pyridazine (pyd)	331[79]	0.32
2,4-pentanedionato (1−, acac)	321[50]	−0.08	pyridine (py)	328[68]	0.25
3,3′-bipyridazine (bpdz)	328[57]	0.30	pyridine, 2-(aminoethyl)	327[50]	0.17
3-amino-1-propene[e]	326[59]	0.13	pyridine, 3,5-dichloro (3,5-Cl$_2$py)	331[80]	0.33
4,4′-bipyridine (4,4′-bpy)	329[37,53]	0.27	pyridine, 4-(dimethylamino) (4-NMe$_2$py)	324[81]	
4,4′-bithiazole (btz)	327[82]	0.20	pyridine, 4-carboxy (4-Hcpy)	331[83]	0.29
acetonitrile (CH$_3$CN)	335[84]	0.34	pyridine, 4-chloro (4-Clpy)	329[81]	0.26
ammonia (NH$_3$)	328*[85]	0.07	pyridine, 4-cyano (4-CNpy)	330*[80]	0.32
benzimidazole (BzIm)	328[I]		pyridine, 4-methyl (4-pic)	327[81]	0.23
benzylamine	326[71]	0.14	pyridine, 4-phenyl (4-Phpy)	327[80]	0.23
biimidazole (BiimH$_2$)[f]	331*[86]		pyridine, 4-$tert$-butyl (4-Bu^{t}py)	327[87]	0.23
bipyrimidine, 4,4-dimethyl[g]	330*[88]		terpyridine (terpy)	325*[57]	
bis(4-pyridyl)acetylene	328[89]	0.27	tetrahydrothiophene (tht)	328[68]	0.30
bis[bis(hydroxymethyl)phosphino]benzene	335[90]		thiocyanato (NCS$^-$)	322[44,91]	−0.06
bromide (Br$^-$)	319[44−46]	−0.22	trifluoroacetate (TFA)$^-$[d]	319*[47]	−0.15
carbon monoxide (CO)	348[37]	0.99	trifluorosulfonate (SO$_3$CF$_3^-$)	327[47]	0.13
chloride (Cl$^-$)	319[44−46]	−0.24	trimethylphosphine (P(Me)$_3$)	331[55]	0.33
$tert$-butyl isocyanide (CNBu^t)	332*[92]	0.36	trimethyl phosphite (P(OMe)$_3$)	339*[92]	
cyanate (NCO$^-$)	316[58,93]	−0.25	tri-n-butylphosphine (P(Bu^n)$_3$)	331[94]	0.29
cyanide (CN$^-$)	318*[95]	0.02	triphenylphosphine (P(Ph)$_3$)	332[47]	0.39
diethyldithiocarbamato (1−)	319[96]	−0.08	triphenyl phosphite (P(OPh)$_3$)[h]	340[97]	0.58
diethylphenylphosphine (PEt$_2$Ph)	336[55]		tritolylphosphine (P(Tol)$_3$)	332[98]	0.37
diethyl sulfide (Et$_2$S)	329[99]	0.35	water	336[52,57,72]	*0.04*

[a] By assuming a ±2 cm^{-1} error in $\nu_{CO^{obs}}$, the estimated error of $IR_P(L)$ parameters = ±0.8 cm^{-1}. [b] E_L value of 1,4,5,8-tap. [c] Derived from n-propyl isocyanide. [d] Derived from comparison with Mn complexes. [e] Derived from ethylamine. [f] Derived from dimethylbiimidazole. [g] Derived from bipyrimidine, 4,4-diphenyl. [h] For a correct prediction of $\nu_{CO^{obs}}$, add 5 cm^{-1} for each ligand coordinated to the metal core. [I] Supporting Information.

against a total of 80 complexes, none of which was used to derive the values (Figure 2 and the Supporting Information). According to the best linear fit through the 81 points plotted in Figure 2, the following equation is derived for *fac*-[Re(CO)$_3$L$_3$] complexes

$$\nu_{CO^{obs}} \text{ (cm}^{-1}) = 1.02[\textstyle\sum IR_P(L)] - 41.6; \; R = 0.99 \quad (5)$$

where $\nu_{CO^{obs}}$ = experimentally observed symmetric C≡O stretching frequency and $\sum IR_P(L)$ = sum of $IR_P(L)$ ligand values.

In Table 1 asterisks indicate values for which inconsistent data are available. As such, these $IR_P(L)$ values may not be well-defined. IR spectra are largely dependent on the medium in which they are recorded. Many authors report that data in solution and solvents vary from water to CCl$_4$. No correction was made to account for variables like the pH, polarity, dielectric constants, or viscosity of the medium. Some data

are only available from in situ experiments (e.g., electrochemical IR experiments), where the presence of an electrolyte or other reagents may influence $\nu_{CO^{obs}}$. Very rarely, the resolution of the spectrum is given. Furthermore, for any given charged complex, $\nu_{CO^{obs}}$ appears to be influenced by the nature of the counterion.

A few examples should illustrate the difficulty of extracting precise IR data from the literature. Schweiger has reported the synthesis of the *fac*-[Re(CO)$_3$(PPh$_3$)$_2$(SO$_3$CF$_3$)] complex and its IR spectrum in both CH$_2$Cl$_2$ and CHCl$_3$.[47] The symmetric C≡O frequency of the complex is observed at 2038 cm^{-1} in CH$_2$Cl$_2$ and at 2046 cm^{-1} in CHCl$_3$. This indicates a difference of 8 cm^{-1} for the same species in two similar solvents. Even more dramatic are differences observed in the IR spectra of tricarbonyl complexes containing cyanide or isocyanide ligands. $\nu_{CO^{obs}}$ values in a KBr pellet
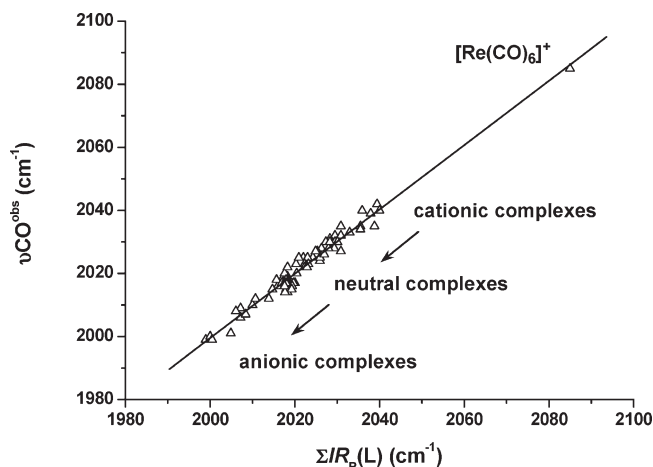
(47) Schweiger, M.; Beck, W. *Z. Anorg. Allg. Chem.* **1991**, *595*, 203–210.

Figure 2. Plot of observed symmetric C≡O stretching frequencies of octahedral *fac*-[Re(CO)$_3$L$_3$] complexes ($\nu_{CO^{obs}}$, *y* axis, cm^{-1}) against $\sum IR_P$(L) (*x* axis, cm^{-1}). The plot shows the linear relationship between $\nu_{CO^{obs}}$ and $\sum IR_P$(L) of 81 complexes. With the exception of [Re(CO)$_6$]$^+$, none of the complexes was used to derive IR_P(L) values.

Figure 3. Plot of IR_P(L) parameters (*y* axis, cm^{-1}) versus their corresponding E_L values (*x* axis, V).

of K$_2$[Re(CO)$_3$(CN)$_3$],[48] [Ni(phen)$_3$][Re(CO)$_3$(CN)$_3$][48] and [AsPh$_4$]$_2$[Re(CO)$_3$(CN)$_3$] are observed at 2020, 2000, and 1994 cm^{-1}, respectively (Supporting Information).

Nevertheless, although some scattering is observed, the correlation between $\nu_{CO^{obs}}$ and $\sum IR_P$(L) (Figure 2) can be considered linear. The relationship appears to be insensitive to the net charge of the complexes. Thus, [Re(CO)$_3$L$_3$]^n species with a net charge *n* varying from 2− to 1+ will fall on the same line. It is generally observed that the higher the negative charge of the complex considered, the higher the probability that $\sum IR_P$(L) will appear on the lower end of the plot in Figure 2.

Raman Correction. It was previously noted that the single $\nu_{CO^{obs}}$ reported in the IR spectrum of [Re(CO)$_6$]$^+$ corresponds to the T$_{1u}$ CO stretching mode rather than the A$_{1g}$ mode. The A$_{1g}$ mode is only Raman-active, and it is expected at ca. 2190 cm^{-1}.[26,49] Considering this value, IR_P(CO) should be corrected from 347.5 to 365 cm^{-1}. The net effect that this correction has on all IR_P(L) values listed in Table 1 is to decrease all parameters by −17.5 cm^{-1}. Because the same correction would be applied to all values, the relative IR_P parameters would not change. Indeed, by application of the Raman correction, the slope and intercept values in eq 5 are unaltered. We have
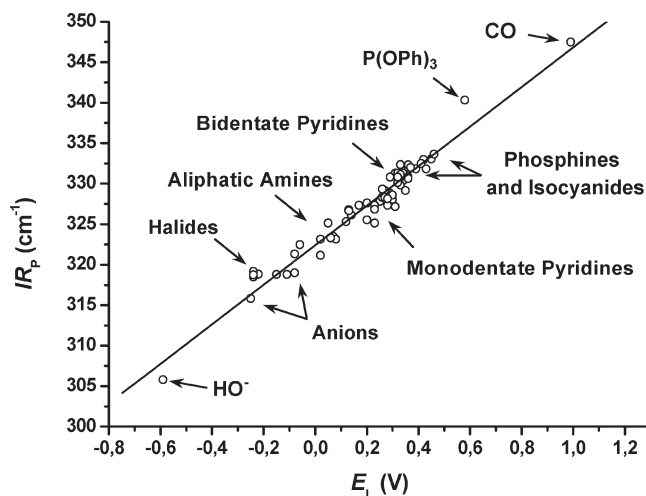
previously emphasized that IR_P(L) ligand values should not be considered in absolute terms.

(48) Behrens, H.; Lindner, E.; Passler, P. *Z. Anorg. Allg. Chem.* **1968**, *361*, 125–133.
(49) Darensbourg, D. J.; Froelich, J. A. *J. Am. Chem. Soc.* **1977**, *99*, 4726–4729.
(50) Benny, P. D.; Fugate, G. A.; Barden, A. O.; Morley, J. E.; Silva-Lopez, E.; Twamley, B. *Inorg. Chem.* **2008**, *47*, 2240–2242.
(51) Herrick, R. S.; Ziegler, C. J.; Cetin, A.; Franklin, B. R. *Eur. J. Inorg. Chem.* **2007**, 1632–1634.
(52) Kurz, P.; Probst, B.; Spingler, B.; Alberto, R. *Eur. J. Inorg. Chem.* **2006**, 2966–2974.
(53) Casanova, M.; Zangrando, E.; Munini, F.; Iengo, E.; Alessio, E. *Dalton Trans.* **2006**, 5033–5045.
(54) Bullock, J. P.; Carter, E.; Johnson, R.; Kennedy, A. T.; Key, S. E.; Kraft, B. J.; Saxon, D.; Underwood, P. *Inorg. Chem.* **2008**, *47*, 7880–7887.
(55) Reimann, R. H.; Singleto, E. *J. Organomet. Chem.* **1973**, *59*, 309–315.
(56) Abel, E. W.; Bhatti, M. M.; Orell, K. G.; Sik, V. *J. Organomet. Chem.* **1981**, *208*, 195–200.
(57) Klein, A.; Vogler, C.; Kaim, W. *Organometallics* **1996**, *15*, 236–244.
(58) Dahlenburg, L.; Hillmann, G.; Ernst, M.; Moll, M.; Knoch, F. *J. Organomet. Chem.* **1996**, *525*, 115–123.
(59) Yang, Y. L.; Chen, J. D.; Lin, Y. C.; Cheng, M. C.; Wang, Y. *J. Organomet. Chem.* **1994**, *467*, C6–C8.
(60) Calderazzo, F.; Mavani, I. P.; Vitali, D.; Bernal, I.; Korp, J. D.; Atwood, J. L. *J. Organomet. Chem.* **1978**, *160*, 207–222.
(61) Horn, E.; Snow, M. R. *Aust. J. Chem.* **1984**, *37*, 35–45.
(62) Lin, R. G.; Fu, Y. G.; Brock, C. P.; Guarr, T. F. *Inorg. Chem.* **1992**, *31*, 4346–4353.
(63) Gibson, D. H.; Yin, X. L. *J. Am. Chem. Soc.* **1998**, *120*, 11200–11201.
(64) Ortega, J. V.; Khin, K.; van der Veer, W. E.; Ziller, J.; Hong, B. *Inorg. Chem.* **2000**, *39*, 6038–6050.
(65) Pietzsch, H. J.; Gupta, A.; Reisgys, M.; Drews, A.; Seifert, S.; Syhre, R.; Spies, H.; Alberto, R.; Abram, U.; Schubiger, P. A.; Johannsen, B. *Bioconjugate Chem.* **2000**, *11*, 414–424.
(66) Abel, E. W.; Bhargava, S. K.; Bhatti, M. M.; Kite, K.; Mazid, M. A.; Orrell, K. G.; Sik, V.; Williams, B. L.; Hursthouse, M. B.; Malik, K. M. A. *J. Chem. Soc., Dalton Trans.* **1982**, 2065–2072.
(67) Alberto, R.; Schibli, R.; Waibel, R.; Abram, U.; Schubiger, A. P. *Coord. Chem. Rev.* **1999**, *192*, 901–919.
(68) Franklin, B. R.; Herrick, R. S.; Ziegler, C. J.; Cetin, A.; Barone, N.; Condon, L. R. *Inorg. Chem.* **2008**, *47*, 5902–5909.
(69) Wrighton, M.; Morse, D. L. *J. Am. Chem. Soc.* **1974**, *96*, 998–1003.
(70) Kirgan, R.; Simpson, M.; Moore, C.; Day, J.; Bui, L.; Tanner, C.; Rillema, D. P. *Inorg. Chem.* **2007**, *46*, 6464–6472.
(71) Fan, J. S.; Lin, J. T.; Chang, C. C.; Chou, S. J.; Lu, K. L. *Organometallics* **1995**, *14*, 925–932.
(72) Lucia, L. A.; Abboud, K.; Schanze, K. S. *Inorg. Chem.* **1997**, *36*, 6224–6234.
(73) Johnson, B. F. G.; Sieker, A.; Blake, A. J.; Winpenny, R. E. P. *J. Organomet. Chem.* **1994**, *475*, 193–200.
(74) Worl, L. A.; Duesing, R.; Chen, P. Y.; Dellaciana, L.; Meyer, T. J. *J. Chem. Soc., Dalton Trans.* **1991**, 849–858.
(75) Gibson, D. H.; Yin, X. L.; He, H. Y.; Mashuta, M. S. *Organometallics* **2003**, *22*, 337–346.
(76) Liddle, B. J.; Lindeman, S. V.; Reger, D. L.; Gardinier, J. R. *Inorg. Chem.* **2007**, *46*, 8484–8486.
(77) Arroyo, M.; Miguel, D.; Villafane, F.; Nieto, S.; Perez, J.; Riera, L. *Inorg. Chem.* **2006**, *45*, 7018–7026.
(78) Ardizzoia, G. A.; LaMonica, G.; Maspero, A.; Moret, M.; Masciocchi, N. *Eur. J. Inorg. Chem.* **1998**, 1503–1511.
(79) Abel, E. W.; Heard, P. J.; Orrell, K. G. *Inorg. Chim. Acta* **1997**, *255*, 65–71.
(80) Giordano, P. J.; Wrighton, M. S. *J. Am. Chem. Soc.* **1979**, *101*, 2888–2897.
(81) Ouh, L. L.; Muller, T. E.; Yan, Y. K. *J. Organomet. Chem.* **2005**, *690*, 3774–3782.
(82) Wolf, M. O.; Wrighton, M. S. *Chem. Mater.* **1994**, *6*, 1526–1533.
(83) Coe, B. J.; Curati, N. R. M.; Fitzgerald, E. C.; Coles, S. J.; Horton, P. N.; Light, M. E.; Hursthouse, M. B. *Organometallics* **2007**, *26*, 2318–2329.
(84) Farona, M. F.; Kraus, K. F. *Inorg. Chem.* **1970**, *9*, 1700–1704.
(85) Zobi, F.; Spingler, B.; Alberto, R. *ChemBioChem* **2005**, *6*, 1397–1405.
(86) Leirer, M.; Knor, G.; Vogler, A. *Inorg. Chim. Acta* **1999**, *288*, 150–153.

Table 2. $IR_P(L)$ Parameter Values (cm^{-1}) Derived from Eq 6

ligand (L)	$IR_P(L)$	E_L	ligand (L)	$IR_P(L)$	E_L
1,10-phenanthroline, 2,9-dimethyl	327	0.2	naphthyridine	328	0.24
1,2,4-triazole	327	0.18	oxalate (2−)	318	−0.17
1,2,4-triazole (1−)	318	−0.17	perchlorate (ClO$_4^-$)	324	0.06
1,2,4-triazole, 4-allyl	325	0.12	phenyl cyanide	331	0.37
1,2,4-triazole, 4-methyl	325	0.11	phenyl cyanide, 3-cyano	333	0.43
1,2,4-triazole, 4-phenyl	326	0.14	phenyl cyanide, 4-chloro	332	0.4
1,3-diphenyl-1,3-propanedionato (1−)	321	−0.04	phenyl cyanide, 4-cyano	334	0.49
1-phenyl-1,3-butanedionato (1−)	321	−0.06	phenyl cyanide, 4-methoxy	331	0.38
2,2′-bipyrazinium (1+)	340	0.75	phenyl cyanide, 4-methyl	331	0.37
2,2′-bipyridine, 4,4′-dibromo	329	0.28	phenyl isocyanide, 2,6-dichloro	333	0.46
3-bromo-2,4-pentanedionato	321	−0.03	phenyl isocyanide, *p*-chloro	331	0.38
3-chloro-2,4-pentanedionato	321	−0.03	phenyl isocyanide, *p*-methoxy	331	0.36
3-iodo-2,4-pentanedionato	321	−0.03	phenyl isocyanide, *p*-methyl	331	0.37
3-methyl-2,4-pentanedionato	319	−0.11	pyridine, 2-(aminomethyl)	325	0.13
3-phenyl-2,4-pentanedionato	320	−0.09	pyridine, 3-(aminomethyl)	325	0.12
acrylonitrile	331	0.38	pyridine, 3,5-dimethyl	327	0.21
azide (N$_3^-$)	315	−0.3	pyridine, 3-carboxamido	328	0.26
benzyl isocyanide	336	0.56	pyridine, 3-iodo	329	0.29
butylamine	325	0.13	pyridine, 4-(trifluoromethyl)	330	0.32
cis-1,2-bis(diphenylphosphino)ethane	334	0.49	pyridine, 4-acetyl	329	0.3
dinitrogen (N$_2$)	339	0.68	pyridine, 4-carbaldehide	330	0.31
ethyl nitrite	339	0.7	pyridine, 4-carboxamido	329	0.28
ethylene	341	0.76	pyridine, 4-cyano (nitrile bonded)	331	0.38
glycine (1−, glyc)	321	−0.05	pyridine, 4-vinyl	327	0.2
imidazole, 4-vinyl	326	0.14	pyrimidine	329	0.29
isonicotinamide	328	0.26	pyrimidinium (1+)	333	0.43
isopropyl nitrite	339	0.68	thiophenolato (1−)	309	−0.53
methyl isocyanide	331	0.37	triethylphosphine	330	0.34
methyl nitrite	340	0.72	trimethyl phosphate	332	0.42
methyl phenyl sulfide	330	0.33	tri *n*-propylphosphine	330	0.34

Comparison of $IR_P(L)$ and E_L Parameters. The usual bonding scheme used to describe an M−C≡O bond invokes σ donation from the ligand to the metal and π back-donation from the metal to the ligand π^* orbitals. This synergistic charge transfer results in (a) an alteration of the electronic density on the metal ion and (b) a decrease of the CO bond order as probed by its frequency in the IR spectrum. By assuming that all ligand contributions are additive and that the symmetric C≡O stretching frequency alone describes the "average electronic environment" in the IR spectra of the complexes, one should find a correlation between $IR_P(L)$ and E_L parameters.

(87) Hori, H.; Ishihara, J.; Koike, K.; Takeuchi, K.; Ibusuki, T.; Ishitani, O. *J. Photochem. Photobiol., A* **1999**, *120*, 119–124.
(88) Ioachim, E.; Medlycott, E. A.; Hanan, G. S. *Inorg. Chim. Acta* **2006**, *359*, 2599–2607.
(89) Sun, S. S.; Anspach, J. A.; Lees, A. J.; Zavalij, P. Y. *Organometallics* **2002**, *21*, 685–693.
(90) Schibli, R.; Katti, K. V.; Volkert, W. A.; Barnes, C. L. *Inorg. Chem.* **2001**, *40*, 2358–2362.
(91) Abram, U.; Hubener, R.; Alberto, R.; Schibli, R. *Z. Anorg. Allg. Chem.* **1996**, *622*, 813–818.
(92) Leins, A. E.; Coville, N. J. *J. Organomet. Chem.* **1994**, *464*, 183–190.
(93) Saillant, R. B. *J. Organomet. Chem.* **1972**, *39*, C71–C73.
(94) Zingales, F.; Trovati, A.; Uguagliati, P. *Inorg. Chem.* **1971**, *10*, 510–513.
(95) Kurz, P.; Spingler, B.; Fox, T.; Alberto, R. *Inorg. Chem.* **2004**, *43*, 3789–3791.
(96) Rowbottom, J. F.; Wilkinson, G. *J. Chem. Soc., Dalton Trans.* **1974**, 684–689.
(97) Bond, A. M.; Colton, R.; Mcdonald, M. E. *Inorg. Chem.* **1978**, *17*, 2842–2847.
(98) Tsubaki, H.; Tohyama, S.; Koike, K.; Saitoh, H.; Ishitani, O. *Dalton Trans.* **2005**, 385–395.
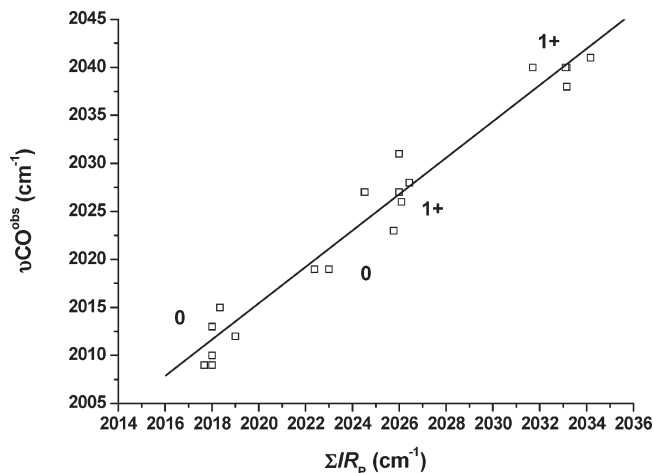(99) Faraone, F.; Sergi, S.; Pietropa, R. *J. Organomet. Chem.* **1970**, *24*, 453–460.

E_L parameters were described by Lever in 1990 as a way of predicting M(n)/M(n−1) redox potentials.[35] A large negative E_L describes a ligand capable of decreasing the potential of the M(n)/M(n−1) redox couple, while a large positive E_L describes a ligand that will have the opposite effect. Because redox processes can be taken as a measure of the electronic density on a metal ion, a negative E_L value describes a ligand with pronounced σ and/or π donation. Thus, a ligand with a negative E_L value should decrease the CO bond order to a higher degree than a ligand with a positive E_L value. This effect, which is a measure of the π back-donation from the metal to the ligand π^* orbitals, should be probed by the shift of the symmetric C≡O stretching frequency to lower reciprocal centimeters. In other words, a negative E_L value should correspond to a low $IR_P(L)$ value.

Of the 92 $IR_P(L)$ values empirically derived, 75 were assigned a E_L parameter. For the comparison between $IR_P(L)$ and E_L, seven of these ligands were not selected because either the $IR_P(L)$ or the E_L value is somewhat variable. Figure 3 shows a plot of $IR_P(L)$ parameters versus E_L values. The correlation is clearly linear, and the relationship between the parameters is given by

$$IR_P(L) \ (\text{cm}^{-1}) = 24.41[E_L] + 322.41; \ R = 0.97 \quad (6)$$

This correlation was then used to derive 60 more $IR_P(L)$ parameters from the E_L value previously published. A complete list is given in Table 2.

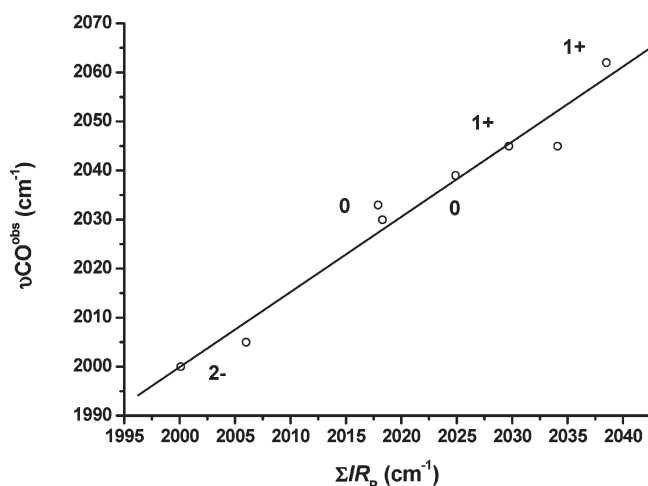**Comparison of $IR_P(L)$ to Other Metal Carbonyl Complexes.** E_L parameters were found to be widely applicable

Figure 4. Plot of observed symmetric C≡O stretching frequencies of octahedral d^6 *fac*-[Mn(CO)₃L₃] complexes ($\nu_{CO^{obs}}$, *y* axis, cm^{-1}) versus $\sum IR_P$(L) (*x* axis, cm^{-1}). The plot shows the linear relationship between $\nu_{CO^{obs}}$ and $\sum IR_P$(L) of 22 complexes. $R = 0.98$, $S_R = 1.89$, and $I_R = -1808.61$ (cm^{-1}). Numbers indicate the net charge of the complexes.
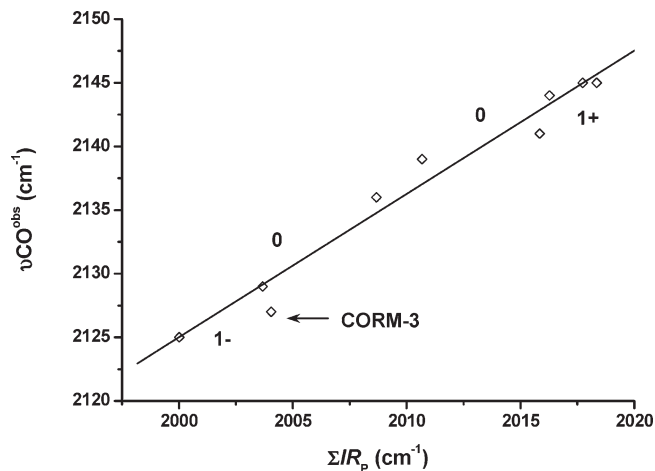

Figure 5. Plot of observed symmetric C≡O stretching frequencies of octahedral d^6 *fac*-[⁹⁹Tc(CO)₃L₃] complexes ($\nu_{CO^{obs}}$, *y* axis, cm^{-1}) versus $\sum IR_P$(L) (*x* axis, cm^{-1}). The plot shows the linear relationship between $\nu_{CO^{obs}}$ and $\sum IR_P$(L) of 8 complexes. $R = 0.98$, $S_R = 1.53$, and $I_R = -1065.28$ (cm^{-1}). Numbers indicate the net charge of complexes.

to many metal ions in different oxidation states.[35,100,101] A linear relationship between IR_P(L) and E_L values points to the general validity of IR_P(L) parameters. To test this hypothesis, the $\sum IR_P$(L) was plotted against $\nu_{CO^{obs}}$ of Mn ⁹⁹Tc, Ru *fac*-[M(CO)₃L₃] complexes, and *cis*-[Re-(CO)₂L₄] species. The least-squares analysis to fit the calculated data to the observed data yields the following equation:

$$\nu_{CO^{cal}} = S_R\left[\sum IR_P(L)\right] + I_R \qquad (7)$$

where $\nu_{CO^{cal}}$ = calculated (or predicted) symmetric C≡O stretching frequency.

(100) Lever, A. B. P. *Inorg. Chem.* **1991**, *30*, 1980–1985.

(101) Lever, A. B. P. Ligand Electrochemical Parameters and Electro-chemical−Optical Relationships. In *Comprehensive Coordination Chemistry II*; Lever, A. B. P., Ed.; Elsevier Pergamon: Amsterdam, The Netherlands, 2005; Vol. *2*, pp 251−268.

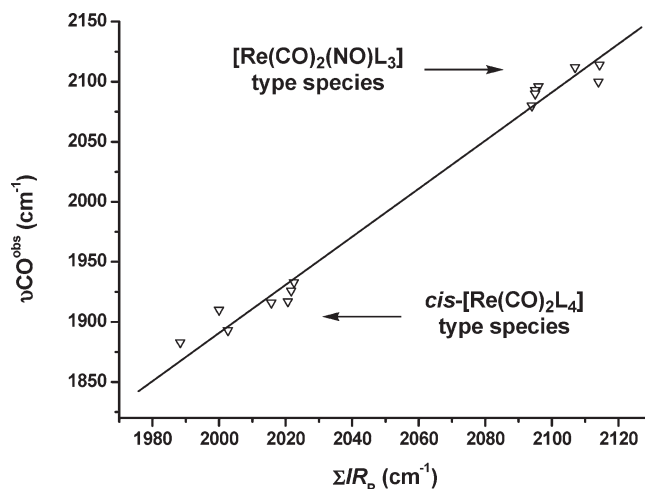**Figure 6.** Plot of observed symmetric C≡O stretching frequencies of octahedral d^6 *fac*-[Ru(CO)₃L₃] complexes ($\nu_{CO^{obs}}$, *y* axis, cm^{-1}) versus $\sum IR_P$(L) (*x* axis, cm^{-1}). The plot shows the linear relationship between $\nu_{CO^{obs}}$ and $\sum IR_P$(L) of 11 complexes. $R = 0.98$, $S_R = 1.13$, and $I_R = -127.25$ (cm^{-1}). Numbers indicate the net charge of complexes.

Figure 7. Plot of observed symmetric C≡O stretching frequencies of octahedral d^6 *cis*-[Re(CO)₂L₄] complexes ($\nu_{CO^{obs}}$, *y* axis, cm^{-1}) versus $\sum IR_P$(L) (*x* axis, cm^{-1}). The plot shows the linear relationship between $\nu_{CO^{obs}}$ and $\sum IR_P$(L) of 15 complexes. $R = 0.99$, $S_R = 2.0$, and $I_R = -2115.6$ (cm^{-1}).

In a fashion directly equivalent to Lever's equation,[35] S_R and I_R are constants that depend upon the metal, its oxidation state, and the number of CO ligands in its primary coordination sphere. Thus, all complexes of given isomerism (i.e., *cis/trans* or *fac/mer*) and spin state and with the same number of CO ligands should fall on the same line. Figures 4−7 show plots of $\sum IR_P$(L) versus $\nu_{CO^{obs}}$ of Mn, ⁹⁹Tc, Ru *fac*-[M(CO)₃L₃] complexes, and *cis*-[Re(CO)₂L₄] species, respectively. Table 3 lists S_R and I_R values of the [M(CO)ₙ] cores, while tables with $\nu_{CO^{cal}}$ and $\nu_{CO^{obs}}$ for the complexes are given in the Supporting Information.
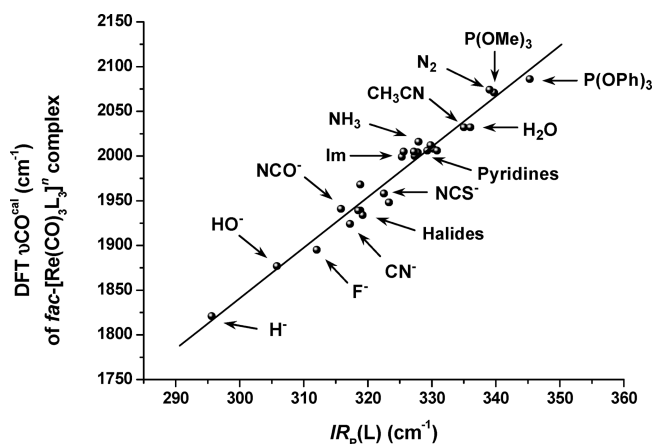
A good correlation is observed in all cases (R = ca. 0.98), but generally $\nu_{CO^{cal}}$ for the *cis*-[Re(CO)₂L₄] species is overestimated. Data plotted in Figure 4−7 were taken from the literature and, with the exception of Mn complexes, no correction was applied for $\nu_{CO^{obs}}$ reported in solution. The relationships, once again, appear to be insensitive to the net charge of the complexes. Thus,

Table 3. S_R and I_R Values of $[M(CO)_n]$ Cores

$[M(CO)_n]$ core	S_R	I_R (cm^{-1})	R^a
fac-$[Mn(CO)_3]^+$	1.89 ± 0.08	-1808.5 ± 165.4	0.98
fac-$[^{99}Tc(CO)_3]^+$	1.53 ± 0.12	-1065.3 ± 250.8	0.98
fac-$[Re(CO)_3]^+$	1.02 ± 0.02	-41.6 ± 39.3	0.98
fac-$[Ru(CO)_3]^{2+}$	1.13 ± 0.07	-127.3 ± 146.7	0.98
cis-$[Re(CO)_2]^+$	2.00 ± 0.07	-2115.6 ± 143.1	0.99

^{a} R = linear regression according to eq 7.

Figure 8. Plot of DFT-calculated symmetric C≡O stretching frequencies (A$_1$ mode) of octahedral fac-$[Re(CO)_3L_3]^n$ complexes (DFT $\nu_{CO^{cal}}$, y axis, cm^{-1}) versus the corresponding $IR_P(L)$ value (x axis, cm^{-1}). The plot shows the linear relationship between DFT $\nu_{CO^{cal}}$ and $IR_P(L)$ of 26 complexes. The $IR_P(CN^-)$ value of 317.2 cm^{-1} was derived from $[AsPh_4]_2[Re(CO)_3(CN)_3]$ (Supporting Information). A 5 cm^{-1} correction was applied to the $IR_P(P(OPh)_3)$ value according to Table 1, footnote h.

species with a net charge n varying from 2− to 1+ fall on the same line. With the exception of ^{99}Tc, complexes containing cyanide, isocyanide (CNR), or PR$_3$ (PR$_3$ = phosphine or phosphite) ligands were not selected in this analysis. These ligands fall within a special class, which will be discussed in more detail later.

Theoretical Evaluation of $IR_P(L)$ Parameters. In order to further verify the validity of the $IR_P(L)$ parameters, these were correlated with the gas-phase $\nu_{CO^{cal}}$ values (i.e., ν_{CO} A$_1$ mode) of different fac-$[Re(CO)_3L_3]^n$ complexes obtained by DFT calculations. Only monodentate ligands were considered in order to directly compare the DFT $\nu_{CO^{cal}}$ values with the corresponding $IR_P(L)$ parameters listed in Table 1 or 2. A total of 26 ligands were selected in order to encompass the widest possible range of $IR_P(L)$ values. These vary from hydride $[IR_P(H^-) = 295.6$ cm$^{-1}]$ to triphenyl phosphite $[IR_P(P(OPh)_3) = 345.3$ cm$^{-1}]$. Figure 8 shows a plot of $IR_P(L)$ versus the DTF $\nu_{CO^{cal}}$ calculated values for the corresponding fac-$[Re(CO)_3L_3]^n$ complex (a table with the actual values is given in the Supporting Information). The good linear relationship observed ($R = 0.98$) further validates the analysis and the empirically determined $IR_P(L)$ values.

Additional analysis of the bond orders and the electronic description of the complexes obtained from the DFT-calculated wave functions has also revealed a good linear relationship between the $IR_P(L)$ parameters and the Re−C and C−O bond orders (NBO) and between the $IR_P(L)$ parameters and the atomic charges (Mulliken) on the carbonyl groups (Figure 9). It appears that in

Figure 9. Top: plot of DFT-calculated average Re−C and C−O bond orders (NBO) of octahedral fac-$[Re(CO)_3L_3]^n$ complexes (y axis) versus the corresponding $IR_P(L)$ value (x axis, cm^{-1}). Bottom: plot of DFT-calculated average Mulliken atomic charges of the $[Re(CO)_3]^+$ core of octahedral fac-$[Re(CO)_3L_3]^n$ complexes (y axis) versus the corresponding $IR_P(L)$ value (x axis, cm^{-1}).

fac-$[Re(CO)_3L_3]^n$ complexes the charge transferred from the three facially arranged L's to the three CO's decreases linearly as the $IR_P(L)$ values increase. Concurrent with higher $IR_P(L)$ values, a linear decrease and increase of the Re−C and C−O bond orders is observed, respectively. These changes are plotted in Figure 9.

Comparison of $IR_P(L)$ and Other Ligand Constants. The first attempt to relate ligand additivity to vibrational spectroscopy was made by Cotton and Kraihanzel.[25−27] They provided a model for assigning CO stretching frequencies of $[M(CO)_{6−n}L_n]$ complexes based on a mathematical evaluation of the C−O force constants. Parameters k_1 and k_2 (ligand force constants) were assigned to ligands cis (k_1) or trans (k_2) to the carbonyl groups, and depending on the point group symmetry of the molecule, different equations were developed.

The Cotton and Kraihanzel's model was later developed by Graham, who further introduced σ and π ligand parameters and showed a linear correlation between these and CO stretching frequencies of $[M(CO)_5L]$ complexes.[28] Because both $IR_P(L)$ and k_1 (or k_2) values are a measure of the ligand additivity probed by vibrational spectroscopy, one should find a linear relationship
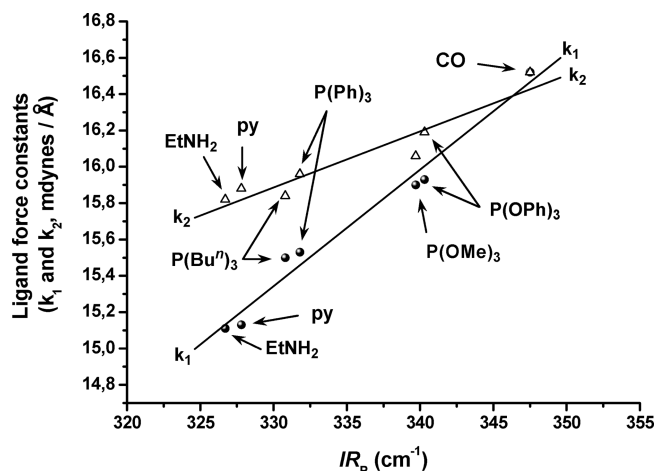
Figure 10. Plot of $IR_P(L)$ parameters (x axis, cm^{-1}) versus corresponding ligand force constants k_1 (dark spheres, $R = 0.99$) and k_2 (open triangles, $R = 0.95$) (y axis, mdyn/Å). k_1 and k_2 values were obtained from ref 28.

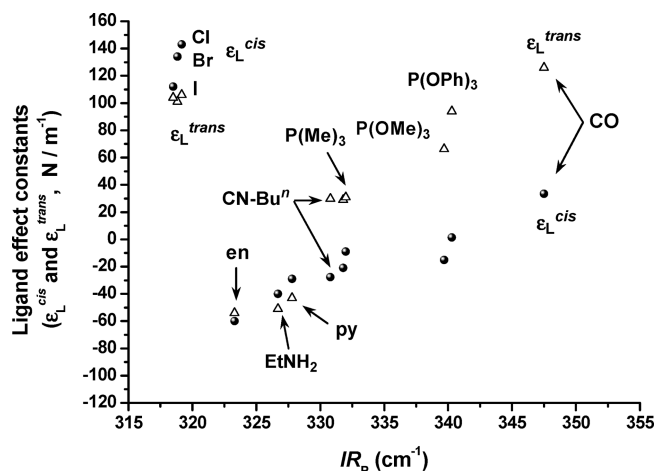**Figure 11.** Plot of $IR_P(L)$ parameters (x axis, cm^{-1}) versus the corresponding ligand-effect constants ε_L^{cis} (dark spheres) and ε_L^{trans} (open triangles) (y axis, N/m).

between these. Figure 10 shows a plot of $IR_P(L)$ parameters versus k_1 and k_2 values.

Indeed, the correlation between the parameters is clearly linear. Although k_1 and k_2 values are known for a number of ligands,[28] not all are assigned an IR_P value. Moreover, in Graham's model, σ and π parameters need to be referenced to a specific ligand (i.e., a ligand must be defined with $\sigma = \pi = 0$ mdyn/Å, in his model either cyclohexylamine or CH_3^-), further reducing the number of common ligands. Thus, only seven points are plotted in Figure 10.

Timney also developed a model based on force constants.[29] He introduced the following simple empirical equation to predict CO stretching frequencies:

$$k_{CO} = k_d + \sum \varepsilon_L^{\theta}$$

where k_d is the force constant of an isolated M(CO) fragment and ε_L^{θ} (called the ligand-effect constant) refers to a ligand L bound to M(CO) at an angle θ. However, we found no correlation between Timney's ε_L^{cis} and

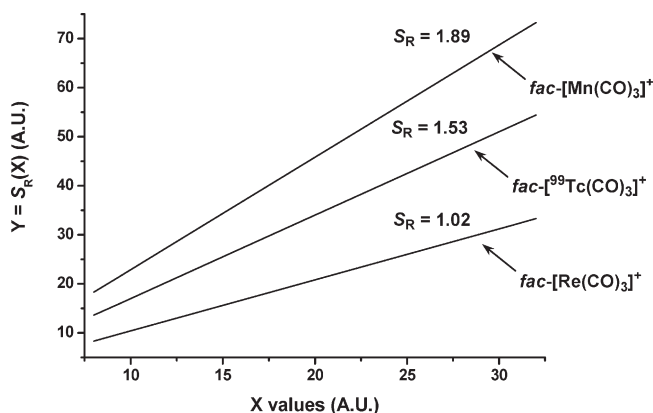**Figure 12.** Comparison of the S_R values of Mn, ^{99}Tc, and Re complexes of the *fac*-[M(CO)$_3$]$^+$ core (A.U. = arbitrary units).

ε_L^{trans} ligand-effect constants and $IR_P(L)$ parameters (Figure 11). Timney's ε_L^{cis} and ε_L^{trans} ligand-effect constants are difficult to interpret from a chemical point of view. The author himself clearly avoided such a discussion. Generally, however, a positive ε_L^{θ} value should indicate a ligand capable of decreasing CO π back-donation, while a negative ε_L^{θ} value should indicate a ligand capable of decreasing the CO bond order. It is, however, difficult to explain why halides have large positive ε_L^{θ} parameters.

Limitations of the Model: CN^-, CNR, and PR$_3$ Ligands. The extent by which the self-consistency of the model holds true was demonstrated in Figure 2. However, when a strong π-acceptor ligand L is coordinated to the metal carbonyl core M, eq 5 generally underestimates ν_{CO}^{obs}. It appears that ligand additivity alone fails to predict strong synergistic interactions between L and M. The difficulty of extracting a precise IR_P value for CN^- was previously illustrated by the limited, and somewhat conflicting, number of data points. Isonitriles (CNR) and PR$_3$ ligands (PR$_3$ = phosphine or phosphite) deserve further comments.

When PR$_3$ ligands are bound to the *fac*-[Re(CO)$_3$]$^+$ core, ν_{CO}^{cal} is, on average, 5 cm^{-1} lower than ν_{CO}^{obs} for these species. There are, however, cases, generally if phosphites are present, when the difference between ν_{CO}^{cal} and ν_{CO}^{obs} is ca. 10 cm^{-1} (i.e., $\nu_{CO}^{obs} > \nu_{CO}^{cal}$). If only PR$_3$ complexes are considered, one finds that the S_R value for the *fac*-[Re(CO)$_3$]$^+$ core increases from 1.02 to ca. 1.4 (Supporting Information). Considerations about the chemical significance of the slope are given in the next section, but one may take this difference as an indication that the model underestimates the extent by which PR$_3$ ligands deplete the electronic density from the metal. Because greater differences between ν_{CO}^{cal} and ν_{CO}^{obs} are generally associated with ligands bearing bulky substituents, distortion of the octahedral environment may also partially explain the discrepancies.

Isonitriles are a very special class of ligands. It was already previously noted that electrochemical parameters associated with CNR's vary significantly from one set of complexes to another.[35,102,103] Often a rather

(102) Doonan, D. J.; Balch, A. L. *Inorg. Chem.* **1974**, *13*, 921–927.
(103) Pombeiro, A. J. L.; Pickett, C. J.; Richards, R. L. *J. Organomet. Chem.* **1982**, *224*, 285–294.

complex fitting procedure needs to be applied to these ligands in order to obtain linear relationships. As was previously suggested,[35] variations in the IR_P (and other) parameters may be attributed to differences in the binding modes of the ligands. When bound to a metal core, CNR's can be linear or bent, with the latter occurring when extensive π back-donation is at play.

Significance of the Slope (S_R) and Intercept (I_R). $IR_P(L)$ parameters describe the electronic effect, or contribution, that any given ligand L will add to a $[MCO_n]$ core in terms of the total observed energy of symmetric C≡O stretching frequencies. The sum of the parameters (i.e., $[\sum IR_P(L)]$) is always constant irrespective of the nature of the $[MCO_n]$ core. Thus, chemical and electronic differences among the $[MCO_n]$ cores considered must reside in the S_R and I_R values. As mentioned before, one of the results of the synergistic charge transfer in an M−CO bond is a decrease of the CO bond order. $\sum IR_P(L)$ probes this effect by assigning a frequency in the IR spectrum. This frequency will always be constant for a chosen set of ligands; thus, the S_R value is a measure of the remaining π back-donation from the metal to the ligand π^* orbitals. In other words, the S_R value is a measure of the M−CO bond strength.

For any given $[M(CO)_n]$ core, a large S_R value will increase the frequency assigned by $[\sum IR_P(L)]$. Thus, a large S_R value indicates bound CO ligands with higher triple-bond character. This points to a reduced π back-donation from the metal to the ligand π^* orbitals and, consequently, to a longer M−CO bond. Therefore, within a set of complexes of given isomerism, spin, and oxidation state and with the same number of CO ligands, the S_R value is directly proportional to the C≡O bond order and inversely proportional to the M−CO bond strength. A comparison of the S_R values of the *fac*-[M-$(CO)_3]^+$ core of the group VII metals is shown in Figure 12. The value decreases when moving down the group (i.e., S_R of Mn > ^{99}Tc > Re), suggesting that the M−CO bond strength increases as one moves from period 4 to 6 (i.e., M−CO bond strength of Re > ^{99}Tc > Mn).

In this analysis, the I_R value is likely to carry additional information about π back-donation relative to the Re system. Suppose that, by chance, comparable complexes with different metals had an identical S_R-$[\sum IR_P(L)]$ value. Then differences in $\nu_{CO^{obs}}$ would arise solely from the I_R intercept. In this case, the lowest frequency species would have the greatest π back-donation. This would indicate that the lower the I_R intercept value, the lower the extent of π back-donation. Indeed, if one considers again the group VII metals, the I_R value follows the order Re > ^{99}Tc > Mn (see Table 3).

IR Ligand Series. Analysis of the IR_P data obtained from the model allows one to compile an IR ligand series that is equivalent to the textbook Dq spectrochemical series and to the E_L series described by Lever.[35] The $IR_P(L)$ ligand parameters in the following sequence should not be considered in absolute terms. They rather should be regarded as a guide to sample from the list ligand types for the design of carbonyl complexes with specific C≡O

stretching frequencies.

$$IR_P(L) : 300 \rightarrow 322 \text{ cm}^{-1}$$
HO$^-$, most anions and strong π bases

With respect to $\nu_{CO^{obs}}$ of $[Re(CO)_6]^+$, substitution of three facial CO's with three of these ligands will cause a shift of $\nu_{CO^{obs}}$ from 143 to 76 cm^{-1} to lower frequency (i.e., $\Delta IR_P = -143 \rightarrow -76 \text{ cm}^{-1}$)

$$IR_P(L) : 322 \rightarrow 332 \text{ cm}^{-1}$$
aliphatic amines, thioethers, pyridines, and bidentate aromatic ligands($\Delta IR_P = -76 \rightarrow -47 \text{ cm}^{-1}$)

$$IR_P(L) : 332 \rightarrow 339 \text{ cm}^{-1}$$
isonitriles, isocyanides, and phosphines
($\Delta IR_P = -47 \rightarrow -26 \text{ cm}^{-1}$)

$$IR_P(L) : 339 \rightarrow 345 \text{ cm}^{-1}$$
phosphites, nitrites, positively charged ligands, and π-acid olefins($\Delta IR_P = -26 \rightarrow -14 \text{ cm}^{-1}$)

$$IR_P(L) : 348 \text{ cm}^{-1}$$
CO
($\Delta IR_P = 0 \text{ cm}^{-1}$, by definition)

$$IR_P(L) : \text{ca. } 440 \text{ cm}^{-1}$$
NO$^+$ (highest $IR_P(L)$ value, may vary significantly)
($\Delta IR_P = +276 \text{ cm}^{-1}$)

Conclusions

A ligand parameter, $IR_P(L)$, was described in order to generate a ligand series that may be used to predict the symmetric C≡O stretching frequency of octahedral metal carbonyl complexes. The parameter, which was empirically derived from *fac*-[Re(CO)$_3$L$_3$] complexes, was obtained under the assumptions that the symmetric C≡O stretching frequency alone describes the "average electronic environment" in the IR spectra of the complexes and that ligand contributions are additive.

The analysis was limited to *fac*-[M(CO)$_3$] cores and to a *cis*-[M(CO)$_2$] core of some metal ions that are currently of general interest in medicinal inorganic chemistry and, in particular, as CORMs. Thus, based purely on thermodynamic considerations, the IR_P parameters should serve as a guide for the design of novel CORMs. Although the available data are limited to Mn, ^{99}Tc, Re, and Ru complexes, the linear relationship between $IR_P(L)$ and E_L values points to the general validity of the $IR_P(L)$ parameters. In principle, an empirical evaluation of the IR data of other $[M(CO)_n]$ cores

should yield S_R and I_R values that may then be used for a specific correlation of $\sum IR_P(L)$ and any given $[M(CO)_n]$ core according to eq 7.

It is certainly clear that the design of potentially useful CORMs cannot simply be reduced to a mathematical summation of the IR_P parameters. It is also obvious that the chemistry of metal carbonyl complexes cannot be anticipated solely from the symmetric stretching frequency of the CO ligands. The *fac*-[RuCl(glycinato)(CO)$_3$] complex (CORM-3), for example, is one of the most promising compounds for CO release in vivo despite the fact that the *fac*-[Ru(CO)$_3$]$^{2+}$ core accommodates two ligands with low IR_P values. Nevertheless, within the set of $[M(CO)_n]$ cores presented, the IR_P parameters allow one to (a) predict the symmetric stretching frequency of a $[M(CO)_n]$ core for any given set of ligands, (b) predict which ligands may comprise the coordination sphere of an $[M(CO)_n]$ core by fitting $\nu_{CO^{obs}}$ to eq 7 given above, (c) provide bonding or structural information (i.e., strong synergistic interactions) where a predicted $\nu_{CO^{cal}}$ is significantly different from $\nu_{CO^{obs}}$, (d) through a comparison of the S_R values within a set of related complexes predict the extent of π backdonation, and (e) derive unknown E_L parameters by fitting $\nu_{CO^{obs}}$ to eq 6.

Supporting Information Available: Tables S1−S6 and Figures S1−S5. This material is available free of charge via the Internet at http://pubs.acs.org.